TÜBİTAK

Turkish Journal of Physics

http://journals.tubitak.gov.tr/physics/

Research Article

Turk J Phys
(2023) 47: 111 – 123

doi:10.55730/1300-0101.2741

Probing exotic neutral current interactions with coherent elastic neutrino-nucleus scattering

Mehmet DEMİRCİ[1,2,*]
[1]Department of Physics, Faculty of Science, Karadeniz Technical University, Trabzon, Turkey
[2]Department of Physics, University of Wisconsin–Madison, Madison, WI, USA

Received: 03.01.2023 • **Accepted/Published Online:** 16.05.2023 • **Final Version:** 21.06.2023

Abstract: The exotic neutral current introduces new interactions beyond standard model (BSM) which consist of all possible four-fermion nonderivative Lorentz structures: scalar (S), pseudoscalar (P), vector (V), axial-vector (A), and tensor (T). In this work, we investigate the prediction of this model via the coherent elastic neutrino-nucleus scattering (CEνNS). The differential cross section spectrum of CEνNS for three nuclei in regards to experiment advancement are calculated in the framework of this model independent proposal using recent obtained bound. We present the ratio of this exotic model with the SM for various threshold energies. Significant bound is shown lie in the lower threshold case. The contributions from exotic neutral current interactions can considerably increase the rate of production relative to the SM case.

Keywords: CEνNS, exotic neutral current, standard model

1. Introduction

The probing of new physics through neutrino interactions with the nucleus has been comprehensively carried out in recent years. In particular, the coherent elastic neutrino-nucleus scattering (CEνNS) in which neutrinos interact with nucleus as a whole [1] has been studied extensively. This process occurs via the exchange of the neutral Z-boson and the scattered nucleus recoil with small energy. The process has the largest cross section compared to other processes with neutrino, but is difficult to witness due to the low energy region where the coherency prevails. Its importance is that it can be used on probing the SM parameters at low momentum transfer [2–4], neutrino electromagnetic properties [5–7], sterile neutrinos [8–10], nuclear physics parameters [11–13], neutrino nonstandard interactions [14–22], astrophysical phenomena [23] as well as dark matter candidate [24].

The first successful observation was recently made using the stopped pion at Oak National Laboratory by COHERENT collaboration [25]. In the COHERENT experiment, the neutrino source originates from decay at rest pions (DAR-π) with energy of several tens of MeV directed towards the CsI[Na] scintillator, producing an energy threshold of 5 keV for Cs [26]. However, the COHERENT experiment used a relatively high-energy neutrino beam compared to reactor neutrinos. Complementary studies at lower energies in the fully coherent regime have not yet been carried out. On the other

*Correspondence: mehmetdemirci@ktu.edu.tr

word, the exact consistency criteria, which lie at the lower nuclear recoil energies of about a few keV and are estimated to be achieved by the sensitive detector reactor neutrino [27], are still not reached. At higher energies, the elastic process, which is suppressed by the inelastic one, recently called inconsistency [28], is broken. To follow these criteria, various experimental advancements have been proposed and are now observing. The DarkSide experiment, which aims to study weakly interacting massive particle (WIMP) dark matter, has an energy threshold of 0.6 keV with liquid Argon target [31]. In other advancement, the TEXONO experiment is set to reach the nuclear threshold of 0.1 keV with the Germanium target [29], and in their last update they successfully reached 0.2 keV [30]. The CONUS experiment is also carried out with reactor neutrinos by using four highly pure germanium semiconductor detectors [32].

Favor to the WIMP dark matter observation, CEνNS process may be produced in direct detection (DD) experiment [33]. The neutrino backgrounds of this process, which is well-measured from neutrino oscillation experiments, are mainly come from solar and atmospheric neutrinos. Direct measurement of CEνNS is so important for this purpose since interaction of dark matter with nucleus uniquely determined as neutrino background cannot be avoided, termed as the neutrino floor. To investigate the true nature of this phenomena, one proposed that the standard neutrino interaction need to be extended so that it includes other possible invariant bilinear combination; scalar (S), pseudo scalar(P), vector (V), axial-vector (A), and tensor (T) [3]. This kind of interactions, since for CEνNS in SM mediated by Z boson, is termed exotic neutral current interactions or simply SPVAT model from the interaction types.

In this work, we calculate the differential cross section of the exotic neutral current model and present its spectrum, as well as the its ratio with SM as an indication of new physics. The proposed exotic interactions is discussed in the next section. The CEνNS on the exotic framework is then presented afterwards. The cross section numerical prediction for several nuclei, in relation with the widely used type in DD experiments [34] is showed later. Finally, the parameter bound predictions for three different energy bounds are given before the conclusion.

2. Analytical formulation of CEνNS

2.1. SM framework

The neutral current interaction allows the low-energy neutrinos of $E_\nu \leq 50$ MeV to interact coherently with neutrons and protons in a nucleus, remarkably increasing the cross section for a large nucleus. Considering the nucleus as a spin-1/2 particle, we can write the SM differential cross section as follows [3]:

$$\frac{d\sigma_{SM}}{dT_N} = \frac{G_F^2 Q_{SM}^2 |F(q^2)|^2 M}{4\pi}\Big(1 - \frac{T_N}{E_\nu} - \frac{MT_N}{2E_\nu^2}\Big), \tag{2.1}$$

where G_F denotes the Fermi coupling-constant, T_N is nuclear recoil energy, E_ν is initial neutrino energy, and M is mass of nucleus. The Q_{SM} denotes the SM weak charge given by

$$Q_{SM} = N - (1 - 4s_W^2)Z, \tag{2.2}$$

where we have defined contribution from the weak angle as $s_W \equiv \sin\theta_W$, while N and Z denote the number of neutron and proton of the involved nucleus, respectively. The updated value of the s_W^2 [35]

is estimated at $(1-4s_W^2)=0.07516$, showing that the process depends quadratically on the number of neutrons for a heavy target nuclei. The charge Q_{SM} describes the vector interaction for the SM which sometimes termed weak-charge. The spin-1/2 case only differs in the last term of the cross section in Eq. (2.1) compared to the spin-0 case, which can be neglected for small T_N. Also we note that this form applies to both neutrino and antineutrino cases, since parity is preserved in Z boson exchange. It is worth noting that we neglected the presence of axial-vector current.

The nucleus recoil energy T_N has a maximal value as follows:

$$T_{Nmax}=\frac{2E_\nu^2}{M+2E_\nu}, \tag{2.3}$$

which depends on E_ν and M, and it can be taken as $2E_\nu^2/M$ for $E_\nu \ll M$. For new physics beyond the SM, Equation (2.1) can be modified but Equation (2.3) still holds since it is obtained directly from relativistic kinematics. A detection threshold T_{th} is placed on T_N for all types of detectors. Hence, for a given E_ν, the recoil energy T_N of detected events should be in the range $T_N \in [T_{th}, T_{Nmax}]$ and the measurable reduced total cross section is given by

$$\sigma_{SM}=\int_{T_{th}}^{T_{Nmax}}\frac{d\sigma_{SM}}{dT_N}dT_N=\frac{G_F^2Q_{SM}^2|F(q^2)|^2M}{4\pi}\frac{1}{2T_{Nmax}}\left[(T_{Nmax}-T_{th})^2\right], \tag{2.4}$$

where the terms proportional to T_N^2/E_ν^2 are neglected.

The $F(q^2)$ is the nucleus form factor which represents the structure of nucleus. It is given as a function of the momentum transfer q where $-q^2\equiv Q^2=2MT_N$. The same form factor is also used for proton and neutron. Since full coherency occurs as $q\to 0$, then $F(q^2)\approx 1$. This shows that the internal configuration of the system is not affected after scattering. This criterion is reached in the realm of small recoil energy. For example in the COHERENT experiment, the observed threshold of Cs nucleus is about 5 keV. Even at this energy, the pure elastic process can be suppressed and breaks the coherent criteria. It is possible the higher energies where neutrino-nucleus interaction still takes place, but now the inelastic process occurs [28]. In the present work, we use the Helm parameterization [36] for the form factor as follows:

$$F(q^2)=\frac{3J_1(qR_0)}{qR_0}e^{-\frac{1}{2}(qs)^2}. \tag{2.5}$$

Here J_1 is the spherical Bessel function of the first order, while $R_0=R^2-5s^2$ is the radius of a nucleus with $R=1.2A^{1/3}$ fm is rms radius and $s=0.5$ fm its thickness. For three different nucleus, the behavior of this form factor as a function of nuclear threshold can be seen in Figure 1. It is clearly depicted that the coherency occurs in the low energy scale and lost this criterion as energy increased. It can also informed that the heavier nuclei tend to suppress the differential cross section quicker than the lighter ones.

2.2. Exotic neutral current framework

The exotic neutral current refers to four-fermion interactions with all the possible Lorentz invariant form. The proper effective Lagrangian correspond to the proposed exotic neutral current can be

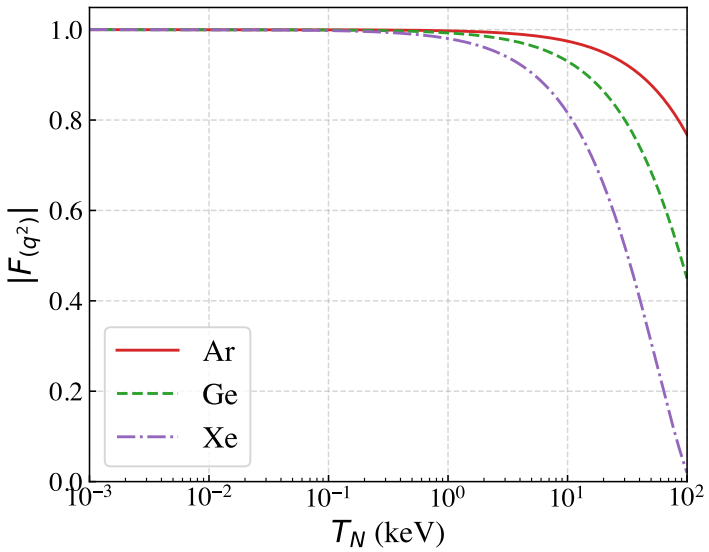

Figure 1. Helm form factor as a function of nucleus recoil energy T_N for Argon, Germanium, and Xenon nuclei.

written in the following form

$$\mathcal{L}_{eff} = \frac{G_F}{\sqrt{2}} \sum_{a=S,P,V,A,T} \bar{\nu}\Gamma^a \nu \bar{N}\Gamma^a (C_a + \bar{D}_a i\gamma^5) N, \tag{2.6}$$

in which a runs from $S, P, V, A,$ to T interactions with

$$\Gamma^a = \left\{ I, i\gamma^5, \gamma^\mu, \gamma^\mu\gamma^5, \sigma^{\mu\nu} = i[\gamma^\mu, \gamma^\nu]/2 \right\}. \tag{2.7}$$

Due to this form, this exotic neutral current is also termed as SPVAT interactions. The ν and N represent neutrino and nucleus spinor, respectively, i.e. proton and neutron are considered to be spin-$1/2$. The parameter C_a and $\bar{D}_a$ denote the vector and axial-vector coefficients of nucleus and contain the quarks interaction. Moreover, only the first generation of quarks are considered and the other heavy possibility as well as gluon contribution is neglected. The detailed relations can be found in Ref. [37] as well as in Appendix C of Ref. [3]. Further detailed calculation that relate the quark couplings in the prescription of chiral theory can be found in Ref. [38]. Comparing the new interaction terms with the standard Fermi theory, their strengths proportional to $\sqrt{2}g_X^2/G_F m_X^2$ where g_X and m_X represent the interaction coupling and mass of the new physics.

We can write the scattering amplitude from the above effective Lagrangian for antineutrino and neutrino cases as

$$\mathcal{M}_{\bar{\nu}N} = -i\frac{G_F}{\sqrt{2}} \bar{\nu}(p_1) P_R \Gamma^a \nu(k_1) \bar{N}(k_2) \Gamma^a (C_a + \bar{D}_a i\gamma^5) N(p_2), \tag{2.8}$$

$$\mathcal{M}_{\nu N} = -i\frac{G_F}{\sqrt{2}} \bar{u}(k_1) \Gamma^a P_L u(p_1) \bar{N}(k_2) \Gamma^a (C_a + \bar{D}_a i\gamma^5) N(p_2), \tag{2.9}$$

respectively. The squared amplitude is constructed by using standard trace techniques. Then, the leading order differential cross section for CE$\nu(\bar{\nu})$NS as a function of nuclear recoil energy is obtained in the following form [3]

$$\begin{aligned}\frac{d\sigma_{EXO}}{dT_N} =& \frac{G_F^2 M N^2}{4\pi}\left[\xi_S^2\frac{MT_N}{2E_\nu^2} + \xi_V^2\left(1-\frac{T_N}{E_\nu}-\frac{MT_N}{2E_\nu^2}\right) + \xi_A^2\left(1-\frac{T_N}{E_\nu}+\frac{MT_N}{2E_\nu^2}\right)\right.\\ &\left. \pm 2\xi_V\xi_A\frac{T_N}{E_\nu} + \xi_T^2\left(1-\frac{T_N}{E_\nu}-\frac{MT_N}{4E_\nu}\right) \pm R\frac{T_N}{E_\nu}\right],\end{aligned} \tag{2.10}$$

where the terms proportional to T_N^2/E_ν^2 are neglected. The positive signs in the $V-A$ and R terms assign neutrino case, while the negative sign is for antineutrino. We note that another form is obtained in Ref. [37], the difference is small as mentioned in the article. All the form factors are included in the parameters $\xi_S, \xi_V, \xi_A, \xi_T$ and R, which are containing the C_a and $\bar{D}_a$. This formulation have reduced the ten free parameters down to five. Explicitly, these exotic parameters are

$$\xi_S^2 = \frac{C_S^2 + D_P^2}{N^2}, \quad \xi_V^2 = \frac{(C_V - D_A)^2}{N^2}, \tag{2.11}$$

$$\xi_A^2 = \frac{(D_V - C_A)^2}{N^2}, \quad \xi_T^2 = \frac{8(C_T^2 + D_T^2)}{N^2}, \tag{2.12}$$

$$R = \frac{2(C_P C_T - C_S C_T + D_P D_T - D_S D_T)}{N^2}. \tag{2.13}$$

We obtain this form by considering spin-1/2 nucleus and compute the amplitude using trace technology in FeynCalc [39]. The ξ_V and ξ_A terms contain the mixture from the vector and axial-vector coefficients, which responsible for the different signs at the T_N/T_{Nmax}. The R term comes from the combination of the tensor and other coefficients. For further use, we introduce a parameter $\vec{\xi} \equiv (\xi_S, \xi_V, \xi_A, \xi_T, R)$. Occurrence of new physics would be clearly indicated if there is a deviation in the ratio of the exotic different cross section with the standard model one. In the next section, this issue will be presented after firstly shown the spectrum behavior of the differential cross section from the model.

3. Numerical predictions and discussion

3.1. Differential cross section

In this section, we present the predictions of the differential cross section spectrum for the CEνNS process in the framework of exotic neutral current. Three benchmark are considered according to different experiment improvement. The first is Argon nuclei that are used by the DarkSide experiment with nuclear threshold energy $T_{th} = 0.6$ keV. The second consideration is Germanium nuclei, considered by the TEXONO collaboration with $T_h = 0.1$ keV aim. The third is from the advancement of COHERENT using Xenon nuclei with $T_{th} = 5$ keV. The standard model case of these three cases provide different vector parameter from the exotic proposal. By comparing Eq. (2.10) with Eq. (2.1) and consider the full coherency, the SM interaction strength satisfies

$$\vec{\xi}_{SM} = \left(0, 1-(1-4\sin^2\theta_W)\frac{Z}{N}, 0, 0, 0\right). \tag{3.1}$$

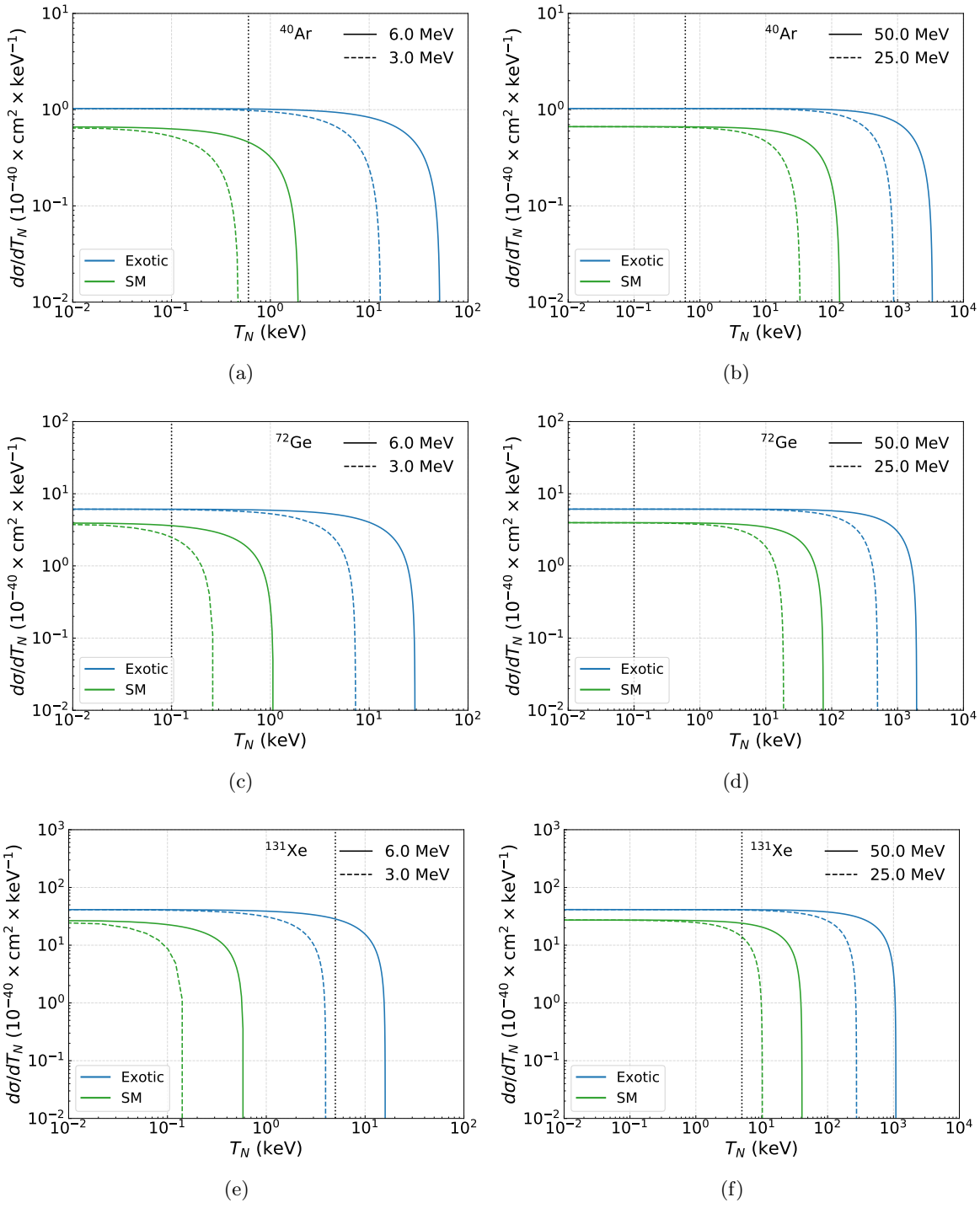

Figure 2. The differential cross section in the framework of the exotic neutral current as a function of T_N for three nuclei with four different initial neutrino energies. The left panel shows the $E_\nu = 3$ and $E_\nu = 6$ MeV while the right panel for $E_\nu = 25$ and $E_\nu = 50$ MeV. The treshold T_N for Ar, Ge, and Xe are $0.6, 0.1$, and 5 keV, respectively.

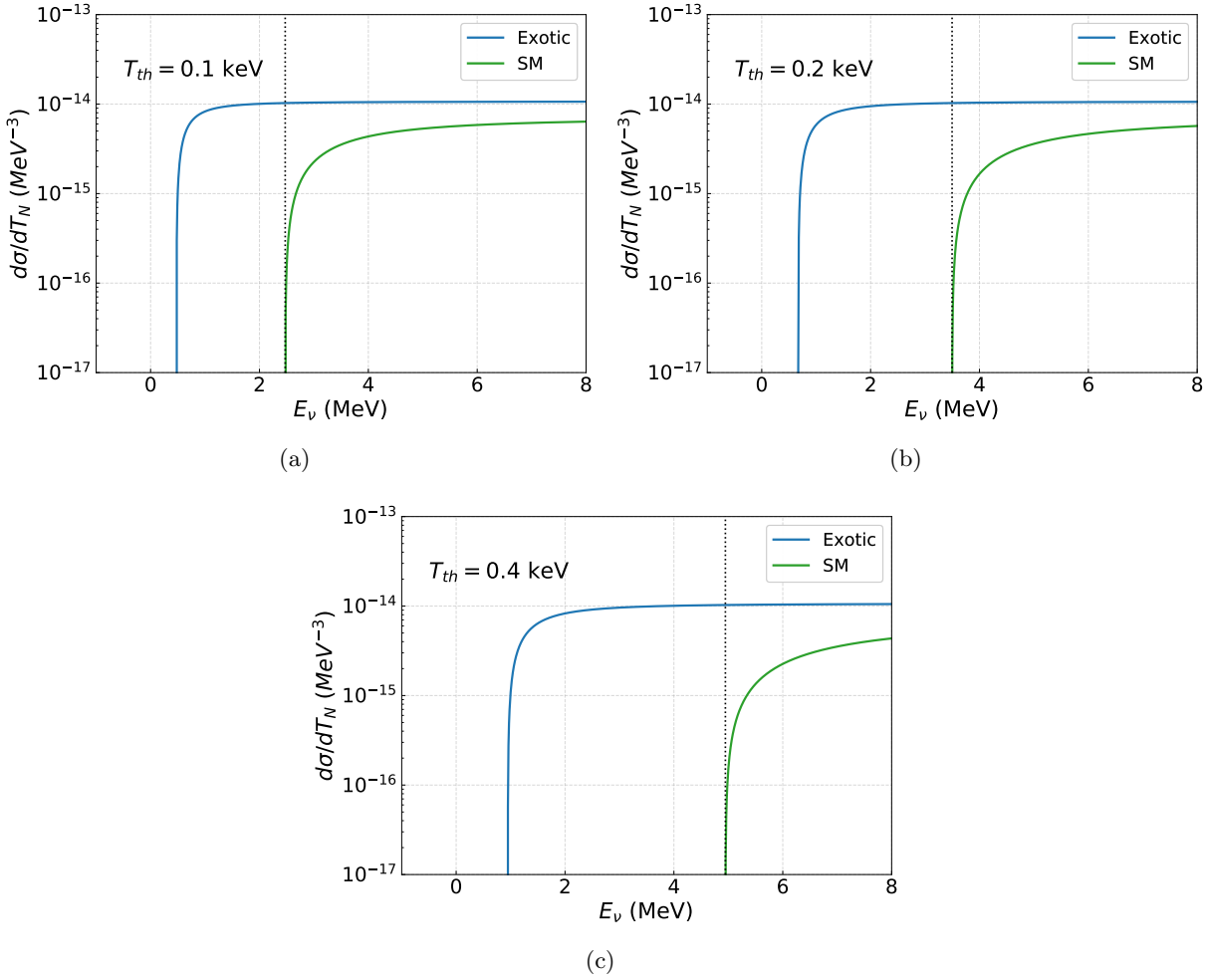

Figure 3. The exotic neutral current differential cross section as a function of neutrino energy E_ν at three different nuclear threshold energy T_{th} for Xenon target. The vertical dotted-lines show the minimum neutrino energies correspond to the T_{th}.

Thus for each considered nuclei, the nonzero value are $0.939, 0.941$, and 0.948 for ^{40}Ar ($Z = 18$), ^{72}Ge ($Z = 32$), and ^{131}Xe ($Z = 54$) nucleus, respectively. Each results from that SM consideration is shown for values within the upper bound values with 99% C.L. of COHERENT data from recent work of Ref. [37]. The values are $\xi_S = 0.9, \xi_V = 0.6$, $\xi_T = 1.0$, and $R = 0$ in which contributions of the psudoscalar and axial-vector have been neglected. For each cases, four different neutrino energies, $E_\nu = 3, 6, 25, 50$ MeV, have been used for illustration. Figure 2 presents the distribution of the differential cross section for each scenario.

Here, we only show the results for the neutrino case. The same results are also obtained for antineutrino case, because the only difference is the sign of the vector axial-vector interference. This is in fact come from assuming the axial-vector interaction is zero. The T_{th} is also shown for each considered experiment advancement plans. The left figures provide the 3 and 6 MeV while the right figures the 25 and 50 MeV neutrino energy cases. Each row respectively gives the spectrum of Argon, Germanium, and Xenon target. As can be seen from these results, Xenon nucleus provides larger

spectrum of differential cross sections than the other targets. It can be seen that the exotic neutral current model provides larger spectrum than the SM case. We notice that slightly different value of interaction strengths could make the spectrum diverge, for example by taking the upper limit of the obtained results in Table 1 of Ref. [37]. This behavior has been anticipated from the different energy dependency in the nonvector interaction terms of Eq. (2.10).

Full coherency contribution occurs as $T_N \to 0$. At lower energy scenario (left panel), the spectrum starts to falls-off at small T_N, around $\lesssim 0.1$ keV. Even for the Xenon nucleus, the coherency suppressed before it reaches 0.2 keV. For higher neutrino energy (right panel), the spectrum is relatively stable until it reaches the 1 keV T_N. Beyond this point, the spectrum slowly decreases. With these both scenarios, the SM predictions show that the higher neutrino energy spectrum (6 and 25 MeV) vanishes after the lower cases (3 and 25 MeV). It is also seen that the SM spectrum vanishes at the low recoil energy than the exotic neutral current.

It can be seen in the lower neutrino energy cases that the spectrum loses its coherency criteria in various T_N scale. The SM case for example, in Figure 2a, the 6 MeV spectrum starts to loss coherency before 0.1 keV and falls-off totally after passing the targeted threshold while the 3 MeV before reaching it, while in Figure 2c, the coherency criteria break also before 0.1 keV and both spectra vanish after the aimed T_{th} passed. In Figure 2e, however, both 3 and 6 MeV cases lose coherency in early T_N and vanish even before reaching the T_{th} target. The exotic spectrum could relatively maintain the coherency criteria after the aimed T_h passed, except for the experiment using Xenon nucleus with 3 MeV neutrino where its spectrum falls before passing its targeted T_{th}. The higher neutrino energy scenario, on the other side, indicates the coherency spectrum could be maintained for relatively higher T_N, around 1 keV, for both SM and exotic cases.

For Xenon nucleus, we provide the effect of exotic neutral current near three different T_{th} $(0.1, 0.2, 0.4$ keV) in Fig. 3. Here the differential cross section of Eq. (2.10) is plotted as a function of E_ν with the same exotic parameters as before. While the SM spectrum vanish at the threshold points, the exotic contribution still dominate and vanish at $E_\nu < 1$ MeV region. These results indicate the occurrence of other types of interaction, predicted by the exotic neutral currents.

3.2. Bound predictions

In this section, we provide the bound predictions from the ratio of exotic with the SM differential cross section for three different T_{th} as shown in Figures 4–6. Here we use the abbreviation of $\sigma_{dif} \equiv d\sigma/dT_N$. The exotic new interaction strengths from this ratio are plotted in parameter space. This method for forecasting new physics has been implemented for CEνNS with NSI framework in Ref. [3]. In every plot, we consider two parameters while set the others to be zero. The implemented three different T_{th} correspond to different bounds. Here the target nucleus is ^{131}Xe with $Z = 54$, at 2.7 MeV initial neutrino energy. The nucleus is used as an advancement to the COHERENT collaboration. Another motivation is from the appealing result of XENON1T experiment that recently foresee the dark matter interaction with Xenon nucleus [40].

In these results, assumption of no interference between scalar and psudoscalar with the tensor interaction, i.e. $R = 0$, has been considered. Notice also that the vector interaction always appears since the same kinematic form of this term with the SM case. The condition where the ratio is equal to 1, or in other words both have the same spectrum, is indicated by the middle line. The two lines with yellow and red colors respectively show the appearance of slightly lesser (0.7) and greater deviation (1.3). The range of ξ parameters is set to lie between $(-1.5, 1.5)$ so that the bound predictions can

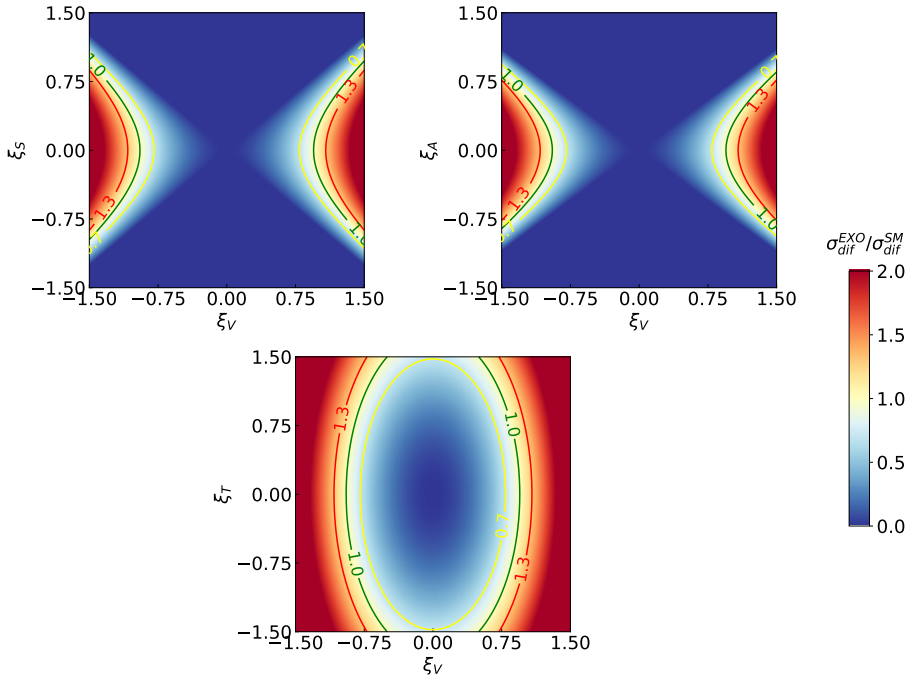

Figure 4. The ratio of $\sigma_{dif}^{EXO}/\sigma_{dif}^{SM}$ on parameter space of exotic neutral current interactions for the nucleus recoil energy threshold $T_N = 0.4$ keV.

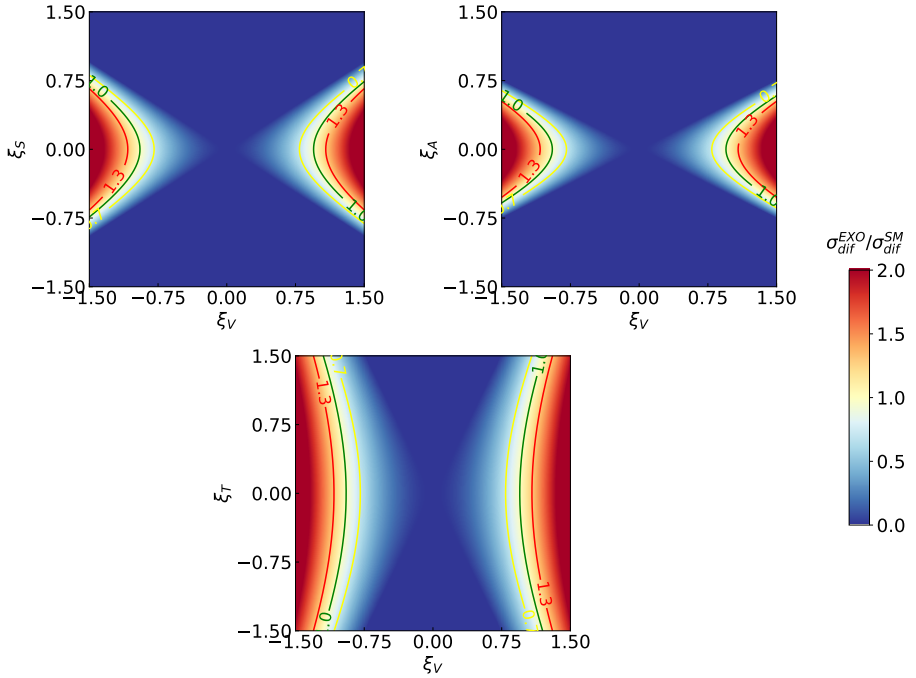

Figure 5. The ratio of $\sigma_{dif}^{EXO}/\sigma_{dif}^{SM}$ on parameter space of exotic neutral current interactions for the nucleus recoil energy threshold $T_N = 0.2$ keV.

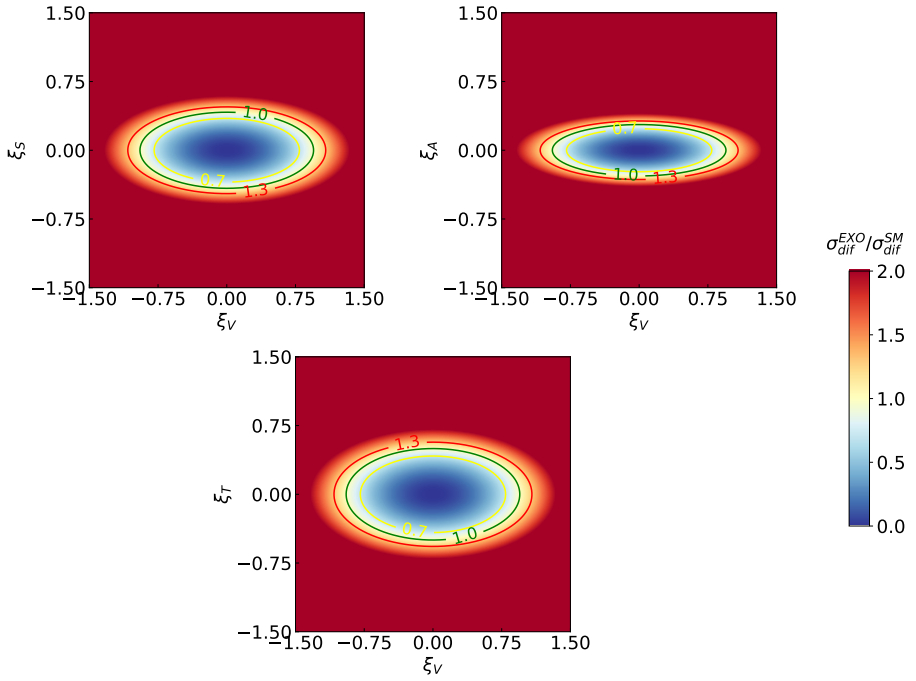

Figure 6. The ratio of $\sigma_{dif}^{EXO}/\sigma_{dif}^{SM}$ on parameter space of exotic neutral current interactions for the nucleus recoil energy threshold $T_N = 0.1$ keV.

be proportionally shown. Greater deviation is occurred in the red region which indicates the exotic spectrum greater than the SM one. Nonsignificant case is shown at the center point where the exotic spectrum has smaller value.

Figures 4–6, respectively, correspond to the modest ($T_{th} = 0.4$ keV), intermediate ($T_{th} = 0.2$ keV), and optimistic bound ($T_{th} = 0.1$ keV), which represent the low-nuclear recoil energy threshold goals in many future advancement of CEνNS experiments. From the modest and intermediate bounds, there are no notable changes on the ξ_V-ξ_S and the ξ_V-ξ_A cases. Significant behavior appears in the optimistic bound where the ellipsoid shapes are formed as the threshold become smaller. A clear deformation can be seen for the ξ_V-ξ_T case in each different energy bound. We emphasize that the region with zero ratio occurs as the interaction from different effective parameter cancels out, namely the region with no new physics can be observed. All these cases would be a clear step to analyze how well the model would fit with the experimental data.

The present work differs from Ref. [3] in terms of our results that give the all 2-dimensional parameter space of the vector interaction with the considered scalar and tensor interaction. The presented contours show the every possible region that can be reached for the given limits.

4. Conclusion

In this work, the exotic neutral current contribution to the CEνNS differential cross section have been presented for several nuclei in regards to the advancement of neutrino experiments. The given numerical results of differential cross sections are slightly in the same order with the SM. The coherent criteria are satisfied in the low energy scale. Spectrum with exotic interactions tends to diverge for the case of heavy nuclei with small incoming neutrino energy. Deviation of the ratio between the

exotic neutral current with the SM differential cross section has been presented as parameter space for each new interaction strengths with three different nuclear recoil energy. Occurrence of small change within those bounds would indicate the existence of new physics, which would be greater than the SM as indicated from the value of the obtained differential cross section predictions. Future CEνNS experiments will provide exciting new data to test SM and new physics beyond SM to unprecedented accuracy. Our results will be beneficial to analyze exotic parameters from future observed data of CEνNS experiment advancements.

Acknowledgment

The work of M.D. was supported by The Scientific and Technological Research Council of Türkiye (TÜBİTAK) in the framework of 2219-International Postdoctoral Research Fellowship Programme.

References

[1] D. Z. Freedman, "Coherent Neutrino Nucleus Scattering as a Probe of the Weak Neutral Current," *Physical Review D* **9** (1974) 1389.

[2] K. Scholberg, "Prospects for measuring coherent neutrino-nucleus elastic scattering at a stopped-pion neutrino source," *Physical Review D* **73** (2006) 033005.

[3] M. Lindner, W. Rodejohann and X. J. Xu, "Coherent Neutrino-Nucleus Scattering and new Neutrino Interactions," *Journal of High Energy Physics* **03** (2017) 097.

[4] J. Barranco, O. G. Miranda and T. I. Rashba, "Probing new physics with coherent neutrino scattering off nuclei," *Journal of High Energy Physics* **12** (2005) 021.

[5] M. Cadeddu, C. Giunti, K. A. Kouzakov, Y. F. Li, A. I. Studenikin, and Y. Y. Zhang, "Neutrino Charge Radii from COHERENT Elastic Neutrino-Nucleus Scattering," *Physical Review D* **98** (2018) 113010.

[6] Yu-Feng Li and Shuo-yu Xia, "Probing neutrino magnetic moments and the Xenon1T excess with coherent elastic solar neutrino scattering," *Physical Review D* **106** (2022) 095022.

[7] A. N. Khan, "Neutrino millicharge and other electromagnetic interactions with COHERENT-2021 data," *Nuclear Physics B* **986** (2023) 116064.

[8] J. M. Berryman, "Constraining sterile neutrino cosmology with terrestrial oscillation experiments," *Physical Review. D* **100** (2019) 023540.

[9] C. Blanco, D. Hooper, and P. Machado, "Constraining sterile neutrino interpretations of the LSND and MiniBooNE anomalies with coherent neutrino scattering experiments," *Physical Review D* **101** (2020) 075051.

[10] O. G. Miranda, D. K. Papoulias, O. Sanders, M. Tórtola, and J.W. F. Valle, "Future CEvNS experiments as probes of lepton unitarity and light sterile neutrinos," *Physical Review D* **102** (2020) 113014.

[11] D. K. Papoulias, T. S. Kosmas, R. Sahu, V. K. B. Kota, and M. Hota, "Constraining nuclear physics parameters with current and future COHERENT data," *Physics Letters B* **800** (2020) 135133.

[12] B. C. Canas, E. A. Garces, O. G. Miranda, A. Parada, and G. Sanchez Garcia, "Interplay between nonstandard and nuclear constraints in coherent elastic neutrino-nucleus scattering experiments," *Physical Review D* **101** (2020) 035012.

[13] M. Cadeddu, F. Dordei, C. Giunti, Y. F. Li, E. Picciau, and Y. Y. Zhang, "Physics results from the first COHERENT observation of coherent elastic neutrino-nucleus scattering in argon and their combination with cesium-iodide data," *Physical Review D* **102** (2020) 015030.

[14] J. Liao and D. Marfatia, "COHERENT constraints on nonstandard neutrino interactions," *Physics Letters B* **775** (2017) 54.

[15] P. B. Denton, Y. Farzan, and I. M. Shoemaker, "Testing large non-standard neutrino interactions with arbitrary mediator mass after COHERENT data," *Journal of High Energy Physics* **07** (2018) 037.

[16] I. Esteban, M. C. Gonzalez-Garcia, and M. Maltoni, "On the determination of leptonic CP violation and neutrino mass ordering in presence of non-standard interactions: present status," *Journal of High Energy Physics* **06** (2019) 055.

[17] A. N. Khan and W. Rodejohann, "New physics from COHERENT data with an improved quenching factor," *Physical Review D* **100** (2019) 113003.

[18] C. Giunti, "General COHERENT constraints on neutrino nonstandard interactions," *Physical Review D* **101** (2020) 035039.

[19] P. Coloma, I. Esteban, M. C. Gonzalez-Garcia, and M. Maltoni, "Improved global fit to Non-Standard neutrino Interactions using COHERENT energy and timing data," *Journal of High Energy Physics* **02** (2020) 023.

[20] L. J. Flores, N. Nath, and E. Peinado, "Non-standard neutrino interactions in U(1)' model after COHERENT data," *Journal of High Energy Physics* **06** (2020) 045.

[21] M. F. Mustamin and M. Demirci, "Study of Non-standard Neutrino Interactions in Future Coherent Elastic Neutrino-Nucleus Scattering Experiments," *Brazilian Journal of Physics* **51** (2021) 813–819.

[22] Yong Du, Hao-Lin Li, Jian Tang, Sampsa Vihonen, and Jiang-Hao Yu, "Exploring SMEFT induced nonstandard interactions: From COHERENT to neutrino oscillations," *Physical Review D* 105 (2022) 075022.

[23] J. R. Wilson, "Coherent Neutrino Scattering and Stellar Collapse," *Physical Review Letters* **32** (1974) 849-852.

[24] A. J. Anderson, J. M. Conrad, E. Figueroa-Feliciano, K. Scholberg and J. Spitz, "Coherent Neutrino Scattering in Dark Matter Detectors," *Physical Review D* **84** (2011) 013008.

[25] D. Akimov et al. [COHERENT Collaboration], "Observation of Coherent Elastic Neutrino-Nucleus Scattering," *Science* **357** (2017) 1123-1126.

[26] D. Akimov et al. [COHERENT Collaboration], "COHERENT Collaboration data release from the first observation of coherent elastic neutrino-nucleus scattering," Zenodo (2018)

[27] S. Kerman et al. [TEXONO Collaboration], "Coherency in Neutrino-Nucleus Elastic Scattering," *Physical Review D* **93** (2016) 113006.

[28] V. A. Bednyakov and D. V. Naumov, "Coherency and incoherency in neutrino-nucleus elastic and inelastic scattering," *Physical Review D* **98** (2018) 053004.

[29] H. T. Wong, "Neutrino-nucleus coherent scattering and dark matter searches with sub-keV germanium detector," *Nuclear Physics A* **844** (2010) 229C.

[30] V. Sharma and H. T. Wong, "Coherency in Neutrino-Nucleus Elastic Scattering," *Journal of Physics: Conference Series* **1468** (2020) 012149.

[31] P. Agnes et al. [DarkSide], "Low-Mass Dark Matter Search with the DarkSide-50 Experiment," *Physical Review Letters* **121** (2018) 081307.

[32] J. Hakenmüller, C. Buck, K. Fülber, G. Heusser, T. Klages et al. "Neutron-induced background in the CONUS experiment," *European Physical Journal C* **79** (2019) 699.

[33] E. Bertuzzo, F. F. Deppisch, S. Kulkarni, Y. F. Perez Gonzalez and R. Zukanovich Funchal, "Dark Matter and Exotic Neutrino Interactions in Direct Detection Searches," *Journal of High Energy Physics* **04** (2017) 073.

[34] J. Billard, L. Strigari and E. Figueroa-Feliciano, "Implication of neutrino backgrounds on the reach of next generation dark matter direct detection experiments," *Physical Review D* **89** (2014) 023524.

[35] R. L. Workman et al. [Particle Data Group], "Review of Particle Physics," *Progress of Theoretical and Experimental Physics* **2022**, 083C01 (2022).

[36] R. H. Helm, "Inelastic and Elastic Scattering of 187-Mev Electrons from Selected Even-Even Nuclei," *Physical Review* **104** (1956) 1466.

[37] D. A. Sierra, V. De Romeri and N. Rojas, "COHERENT analysis of neutrino generalized interactions," Physical Review D **98** (2018) 075018.

[38] F. Bishara, J. Brod, B. Grinstein and J. Zupan, "Chiral Effective Theory of Dark Matter Direct Detection," *Journal of Cosmology and Astroparticle Physics* **02** (2017) 009.

[39] R. Mertig, M. Bohm and A. Denner, "FEYN CALC: Computer algebraic calculation of Feynman amplitudes," *Computer Physics Communications* **64** (1991) 345-359.

[40] E. Aprile *et al.* [XENON Collaboration], "Excess Electronic Recoil Events in XENON1T," *Physical Review D* **102** (2020) 072004.